

Nitridation Reaction of Titanium Powders by 2.45 GHz Multimode Microwave Irradiation using a SiC Susceptor in Atmospheric Conditions

Authors:

Jun Fukushima, Keiichiro Kashimura, Hirotsugu Takizawa

Date Submitted: 2020-02-03

Keywords: on demand process, SiC susceptor, titanium nitride, microwave processing

Abstract:

A titanium nitride (TiN) coating using microwaves can be accomplished in air, and satisfies the required conditions of an on-demand TiN coating process. However, the coating mechanism using microwaves is not completely clear. In this study, to understand the detailed mechanism of microwave titanium nitridation in air, the quantity of nitrogen and oxygen in reacted TiN powder has been investigated by an inert melting method. Titanium powders were irradiated with microwaves by a multi-mode type 2.45 GHz microwave irradiation apparatus, while also being held at various temperatures for two different dwell times. X-ray diffraction (XRD) results revealed that nitridation of the powder progressed with increasing process temperature, and the nitridation corresponds to the powder color after microwave irradiation. The nitrogen contents of the samples increased with increasing processing temperature and dwell time, unlike oxygen. It is postulated that the reaction of convected air with titanium is a key role to control nitridation in this system.

Record Type: Published Article

Submitted To: LAPSE (Living Archive for Process Systems Engineering)

Citation (overall record, always the latest version):

LAPSE:2020.0175

Citation (this specific file, latest version):

LAPSE:2020.0175-1

Citation (this specific file, this version):

LAPSE:2020.0175-1v1

DOI of Published Version: <https://doi.org/10.3390/pr8010020>

License: Creative Commons Attribution 4.0 International (CC BY 4.0)

Article

Nitridation Reaction of Titanium Powders by 2.45 GHz Multimode Microwave Irradiation using a SiC Susceptor in Atmospheric Conditions

Jun Fukushima ^{1,*} , Keiichiro Kashimura ² and Hirotsugu Takizawa ¹¹ Graduate School of Engineering, Department of Applied Chemistry, Tohoku University, Sendai, Miyagi 980-8579, Japan; takizawa@aim.che.tohoku.ac.jp² College of Engineering, Chubu University, Kasugai, Aichi 487-8501, Japan; kashimura@isc.chubu.ac.jp

* Correspondence: fukushima@aim.che.tohoku.ac.jp; Tel.: +81-22-795-7226

Received: 20 November 2019; Accepted: 20 December 2019; Published: 21 December 2019



Abstract: A titanium nitride (TiN) coating using microwaves can be accomplished in air, and satisfies the required conditions of an on-demand TiN coating process. However, the coating mechanism using microwaves is not completely clear. In this study, to understand the detailed mechanism of microwave titanium nitridation in air, the quantity of nitrogen and oxygen in reacted TiN powder has been investigated by an inert melting method. Titanium powders were irradiated with microwaves by a multi-mode type 2.45 GHz microwave irradiation apparatus, while also being held at various temperatures for two different dwell times. X-ray diffraction (XRD) results revealed that nitridation of the powder progressed with increasing process temperature, and the nitridation corresponds to the powder color after microwave irradiation. The nitrogen contents of the samples increased with increasing processing temperature and dwell time, unlike oxygen. It is postulated that the reaction of convected air with titanium is a key role to control nitridation in this system.

Keywords: microwave processing; titanium nitride; SiC susceptor; on demand process

1. Introduction

Titanium nitride (TiN) has a rock salt structure and exhibits high electrical conductivity, high chemical stability and a low diffusion coefficient [1–12]. Therefore, it is used as a diffusion barrier to prevent electromigration, which is a deterioration phenomenon between wiring materials on semiconductor substrates [13–16]. In addition, it has high Vickers hardness, a beautiful gold color and excellent wear resistance, and as a coating film it is widely applied to cutting tools, clinical dentistry and decorative products [17–21].

Recently there has been a market for on-demand processing in small lots for the TiN coating of drills, cutting tools and dental implant materials [22]. However, conventional TiN coating processes, such as chemical vapor deposition (CVD) or physical vapor deposition (PVD), are difficult to apply as a small lot process, due to high processing costs and long processing times. Moreover, CVD and PVD processes are not suitable for the uniform coating of materials with complex shapes. Takizawa et al. have developed a new TiN coating technique in which substrate materials embedded in metallic titanium powder are irradiated with microwaves [23]. This technique can be performed in air using a general-purpose device such as a microwave oven. Consequently, this microwave TiN coating method could be utilized as an on-site TiN coating process.

Nitridation of titanium powders using 28 GHz microwaves in air [24] is the underlying technique of microwave TiN coating. Similarly, Ti–Cr alloy nitriding at atmospheric pressure by 2.45 GHz microwaves has been reported [25]. However, the mechanism of titanium nitridation using microwaves in air is not completely clear.

Metal powders can absorb microwaves [26–28] and the temperature of titanium powders may reach several hundred degrees Celsius in a few minutes. At high temperatures, a gas–solid reaction proceeds in a self-combustion manner, as the heat of formation is large. The change of the Gibbs free energy is negative when titanium metal reacts with nitrogen at room temperature; thus, the reaction progresses spontaneously with sufficient energy exceeding the activation energy. However, the absolute value of the change of the Gibbs free energy of oxidation is larger than that of nitridation. In particular, under thermal equilibrium conditions, titanium powder forms titanium oxides. However, in the microwave process, titanium powder become TiN under air conditions, and these reaction conditions are different from the equilibrium state.

To understand the detailed mechanism of nitridation mechanism, it is necessary to quantify the amount of nitrogen and oxygen in reacted TiN powder. In this study, the nitrogen and oxygen content in titanium nitride were investigated by an inert melting method, and the mechanism of microwave titanium nitridation is discussed.

2. Materials and Methods

2.1. Sample Setting

Figure 1 shows a schematic view of the sample setting. Unprocessed titanium powder (2.0 g; 45 μm pass, Kojundo Chemical Laboratory Co., Ltd., Saitama, Japan) was lightly packed into a quartz tube ($\varnothing 10$ mm OD and $\varnothing 8$ mm ID) sealed at each end with silica wool. Carborundum (SiC) coarse particles were used as the susceptor. The size of the quartz tube is enough to apply a TiN coating to a dental abutment.

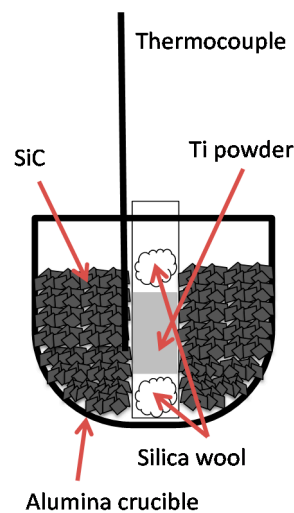


Figure 1. Schematic view of the titanium powder and the SiC susceptor setting within the alumina crucible.

2.2. Microwave Processing

A multi-mode type 2.45 GHz microwave irradiation apparatus (μ Reactor Ex, Shikoku Keisoku Kogyo Co., Ltd., Kagawa, Japan) was used as a microwave furnace. Titanium nitride was synthesized at various temperatures and dwell times. The heating rate was set to 100 $^{\circ}\text{C}/\text{min}$ up to 450 $^{\circ}\text{C}$ and 50 $^{\circ}\text{C}/\text{min}$ after that to prevent thermal runaway of the titanium powder. The temperature was measured using a thermocouple in contact with the center of the test tube. After heating, the quartz tube was immediately removed from the microwave furnace and cooled in air.

2.3. Sample Analysis

The phase of the synthesized samples was analyzed using X-ray diffraction (XRD), and the amount of oxygen and nitrogen contained in the sample was quantitatively analyzed by an inert gas melting method.

Oxygen and nitrogen in titanium metal were quantified by an inert gas melting method (TC600, manufactured by LECO Japan Co.). In the inert gas melting method, titanium metal was heated and melted in an inert gas atmosphere, and released oxygen and nitrogen are quantified (where oxygen detection was conducted by infrared absorption method (JIS H1620), nitrogen detection by heat conduction method (JIS H1612)). The titanium nitride obtained in this study has a nitrogen content higher than the quantitative range defined by JIS (0.005–0.03%). Therefore, the weight of the sample was reduced to ensure the accuracy of the measurement results, and the accuracy was 0.001 wt %.

3. Results

Figure 2 shows the time dependence of the temperature and microwave output power in an experiment at a holding temperature of 950 °C, for a microwave power level of approximately 200 W. The microwave power was Proportional-Integral-Derivative (PID)-controlled, and the sample temperature was controlled as well. However, the microwave power profile exhibited a pulsed behavior, as the microwaves are radiated from a rotary antenna; thus, the microwave distribution in the furnace, the power profile and the heating efficiency, also oscillated.

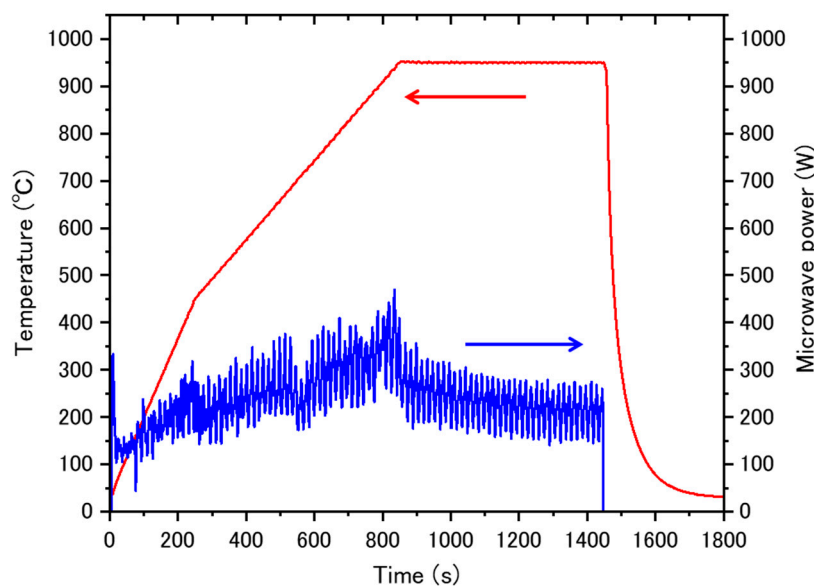


Figure 2. Time dependence of temperature and microwave output power versus time in an experiment at a holding temperature of 950 °C, as shown by the red curve with the red arrow pointing to the left ordinate. The microwave power is shown by the blue curve with the blue arrow pointing to the right ordinate.

Figure 3 shows photographs of the Ti powder for ten samples after microwave irradiation for either 1 min or 10 min while held at one of five temperatures between 800 °C and 1000 °C. The powders became golden colored, indicating that the samples include titanium nitride at each temperature. As the holding temperature increased, the golden color became darker. In contrast, the color of the powders in contact with the silica wool was gray to purple. This suggests that the top and bottom regions of the powders were exposed to convective air and oxidized.

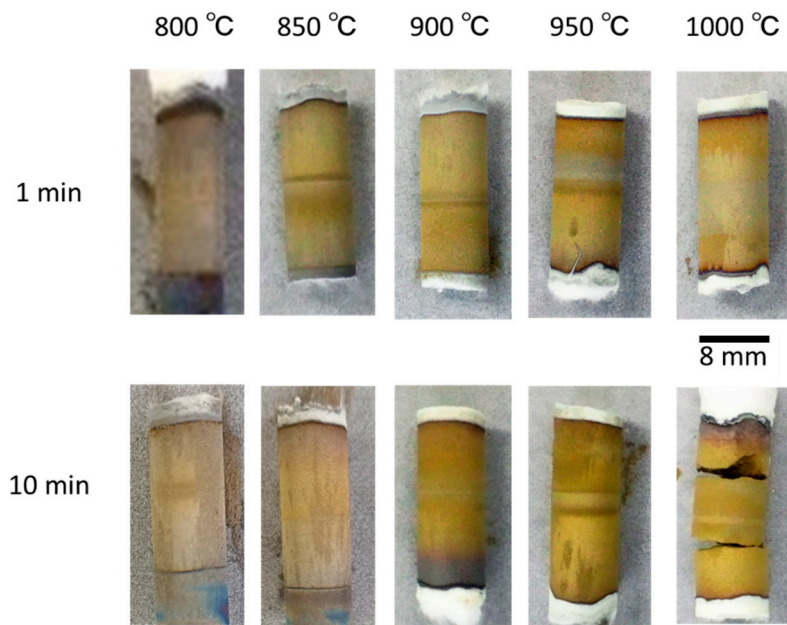


Figure 3. Photographs of the Ti powder after microwave irradiation, for ten samples.

Figure 4a shows the X-ray diffractometry (XRD) results for each sample after microwave irradiation for 1 min. At 800 °C, the main phase consisted of titanium nitride with a low nitrogen content, and the peak intensity of titanium (at around 40 °C) was also large. The sample also included Ti_2N and TiN, but with small peak intensities. The intensity of the titanium and Ti_2N peaks decreased with increasing process temperature. In contrast, the intensity of the TiN peaks increased with increasing process temperature. At a holding temperature of 950 °C or higher, the peak of the pristine titanium almost disappeared. Figure 4b shows the XRD result for each sample after holding for 10 min. As with the 1 min holding duration, the TiN peaks increase in intensity with increasing process temperature. Unlike the 1 min hold time samples, the peak of pristine titanium disappeared completely, and TiN became the main phase in the samples held for 10 min at 950 °C or higher.

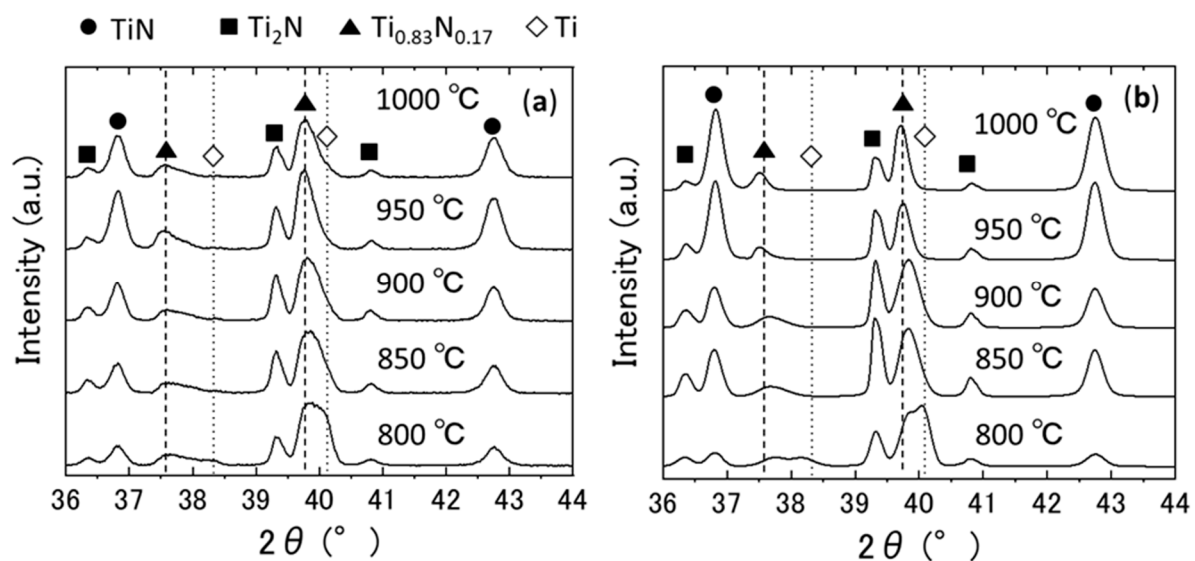


Figure 4. (a) X-ray diffractometry (XRD) results of the sample after microwave irradiation for 1 min. (b) XRD results of the sample after microwave irradiation for 10 min.

Figure 5 shows the oxygen and nitrogen content of the post-experiment samples under each processing condition. The analyzed powder was from the center of the cylindrical sample, in the longitudinal direction. Figure 5a,c indicate that the oxygen content was not significantly different even when the holding temperature and the dwell time increased. In contrast, the nitrogen content tended to increase as the temperature or dwell time increased. The results are consistent with the color analysis—the powder color was darker with increasing temperature and time.

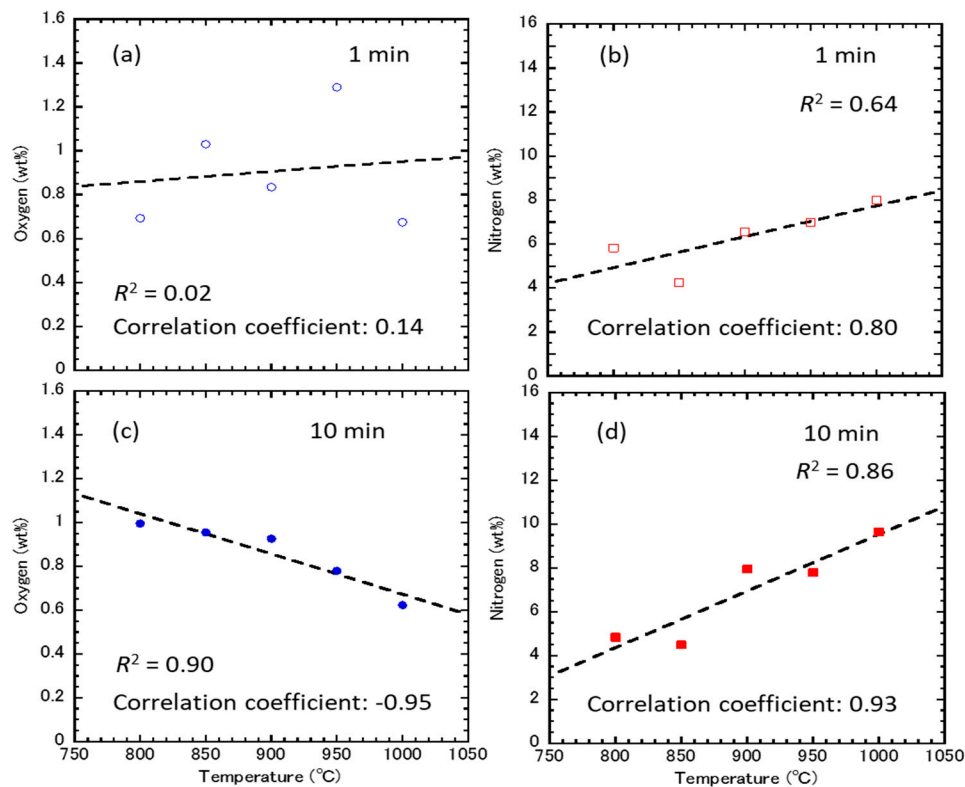


Figure 5. Oxygen and nitrogen content of the post-experiment samples under each processing condition: (a) oxygen for 1 min; (b) nitrogen for 1 min; (c) oxygen for 10 min; (d) nitrogen for 10 min.

The correlation coefficients between the O or N content and temperature are also indicated in Figure 5. The correlation between the oxygen content and the temperature for the 10 min samples was negative, while there was no significant correlation for the 1 min samples. The correlation coefficient between the nitrogen content and temperature was 0.8 or more for both dwell times, indicating that they have a strong correlation. In brief, the nitrogen content of the powder around the center of the test-tube increased as the temperature increased, but the oxygen content either did not change, or it decreased as the temperature and time increased.

The weight ratios of the oxygen and nitrogen in the samples are summarized in Table 1. For the samples with 10 min dwell times, the oxygen (wt %): nitrogen (wt %) proportion was approximately 1:5 for temperatures up to 850 °C. In air, the oxygen (wt %): nitrogen (wt %) proportion is 2:7. Thus, the nitrogen content was higher than for air's composition, even when processing at a relatively low temperature. Above 850 °C, the ratio of the nitrogen content increased as the holding temperature increased. This is due to the increasing nitrogen content and decreasing oxygen content with increasing processing temperature. For the samples with 1 min dwell times, the ratio of oxygen (wt %): nitrogen (wt %) at 800 °C was approximately 2:17, but decreased to 2:9 at 850 °C. Above 900 °C, no temperature dependence of the ratio of nitrogen and oxygen content was observed. As the variation in oxygen content was large for the 1 min dwell times, it indicates that the ratio of nitrogen and oxygen content varied at each temperature.

Comparing the weight ratios of the 1 min and 10 min hold time samples, the nitrogen content ratio for the 10 min samples was larger at all temperatures except 800 °C. This is mainly because the nitrogen content increased with increasing dwell time. In contrast, at 900 °C or lower the oxygen content (wt %) increased with increasing dwell time. In particular, the oxygen content (wt %) at 800 °C for 1 min was larger than with the 10 min dwell time. At 900 °C or higher, the nitrogen content (wt %) increased notably due to an increasing reaction rate at elevated temperatures. Regardless, the ratio of nitrogen content was larger than the atmospheric composition ratio, suggesting that the powder from the center of the sample preferentially reacted with nitrogen in the convected air.

Table 1. Weight ratio of oxygen and nitrogen in the samples.

Time (min)	Temperature (°C)	Oxygen (wt %)	Nitrogen (wt %)	O:N
1	800	0.692	5.82	2:16.8
1	850	1.03	4.26	2:8.3
1	900	0.835	6.57	2:15.7
1	950	1.29	6.97	2:10.8
1	1000	0.675	7.99	2:23.7
10	800	0.996	4.84	2:9.7
10	850	0.956	4.49	2:9.4
10	900	0.927	7.95	2:17.2
10	950	0.78	7.79	2:20.0
10	1000	0.624	9.65	2:30.9

4. Discussion

Based on the above results, we consider the mechanism of the nitridation reaction in this system. It appears that all of air remaining between the powder grains reacted below 800 °C, as the ratio of nitrogen content in the powder at 800 °C was already larger than that of air. Then, convected air was throughout the quartz tube, but the results show that longer dwell times resulted in a decreasing amount of oxygen. Under thermal equilibrium conditions, titanium oxides systems are more stable than titanium nitrides, and thus it is considered that the amount of oxygen increases with longer dwell times. This contradictory result is due to the experimental setup for the powder.

Convected oxygen is presumed to react with titanium powder at the uppermost or the lowermost parts of the test tube; therefore, the nitrogen partial pressure is higher than that of the air, and the nitrogen content of the powder at the central part of the test tube increased. Furthermore, it is postulated that convected nitrogen could reach the center through the powder, as the reaction rate of nitridation is relatively slow compared to oxygen. Further, since the nitridation ratio increased with increasing process temperature, the nitrogen content at the center increased as the holding temperature increased. Accordingly, the natural convection velocity is not thought to be large, as no dramatic increase of the nitrogen content was observed for the 1 min dwell time. With longer dwell time, the nitrogen content of the sample increased due to the increase in the amount of convected nitrogen. The nitridation of titanium powder in this system proceeds as shown in Figure 6.

Conversely, the oxygen content of the sample reduced with increasing temperature for the 10 min dwell time samples. The oxygen partial pressure at the center of the test tube was lower as oxygen reacted with the titanium powder at the uppermost or the lowermost parts of the test tube. In addition, reduction of TiO₂ is promoted under microwave irradiation [29,30] and the reduction of other transition-metal contained oxides was enhanced [31,32], which is due to specific microwave effects [33]. Thus, titanium oxides were reduced, and the reduction rate increased when the processing temperature increased. From the above, the main mechanism for the increase of the nitrogen content ratio in this system is that the nitrogen content increased through reactions with convected nitrogen, and the oxygen content decreased under low oxygen pressure due to oxidation of the titanium powder at the uppermost or the lowermost part of the test tube. Although the above conditions can be obtained by using a conventional furnace, microwaves can rapidly heat the titanium powders via

internal heating. In addition, the heated sample can easily be removed from the microwave furnace and quenched in air. These features of microwave processing result in an efficient nitridation of titanium powders.

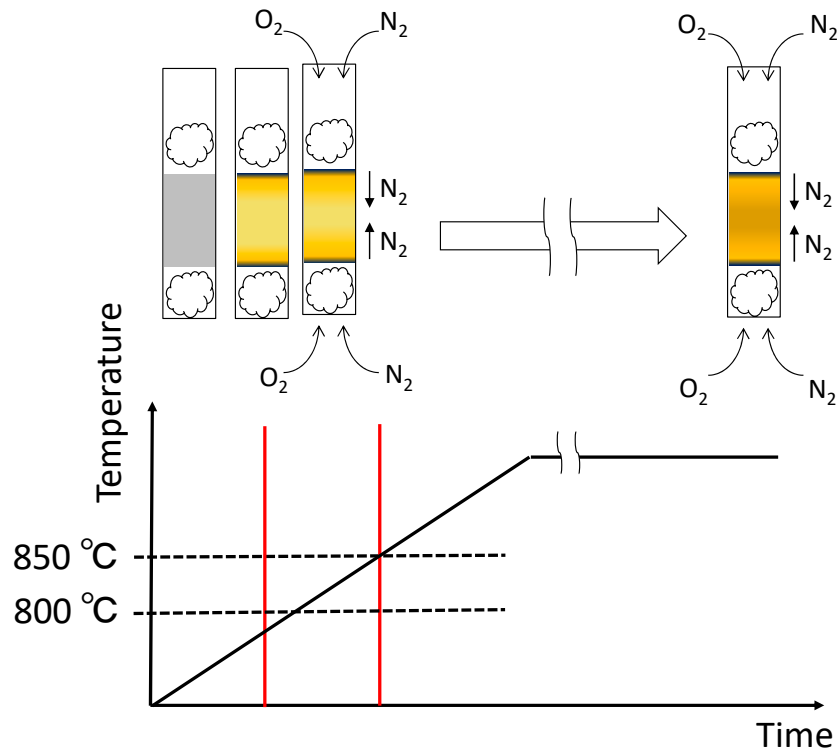


Figure 6. Nitridation behavior of titanium powders under microwave irradiation in this system.

5. Conclusions

This study investigated the nitrogen and oxygen contents of microwave-irradiated titanium powder at various temperatures and times by an inert melting method. The oxygen contents of the sample powder had no correlation with processing temperature for a 1 min duration irradiation, but the nitrogen contents had a positive correlation. In contrast for a 10 min duration irradiation, the nitrogen contents also had a positive correlation, but the oxygen content decreased with increasing process temperature. In this system, convected air first reacted with the titanium powder at the uppermost or the lowermost parts of the test tube, and the partial pressure of nitrogen and oxygen changed from the equilibrium condition. It is postulated that this is the main mechanism responsible for increasing the nitrogen content ratio in this system with increasing process temperature.

Author Contributions: Conceptualization, J.F. and K.K.; Methodology, J.F. and K.K.; Validation, J.F., K.K. and H.T.; Formal Analysis, J.F.; Investigation, J.F.; Resources, K.K. and H.T.; Writing—Original Draft Preparation, J.F.; Writing—Review & Editing, J.F., K.K. and H.T.; Visualization, J.F.; Supervision, K.K. and H.T.; Project Administration, J.F.; Funding Acquisition, J.F., K.K. and H.T. All authors have read and agreed to the published version of the manuscript.

Funding: This research was funded by a JSPS Grant-in-Aid for Scientific Research (S) No. JP17H06156.

Acknowledgments: This work was supported by a JSPS Grant-in-Aid for Scientific Research (S) No. JP17H06156. The authors thank NIPPON STEEL TECHNOLOGY Co., Ltd. for assistance with the inert gas melting method.

Conflicts of Interest: The authors declare no conflict of interest.

References

1. Rebenne, H.E.; Bhat, D.G. Review of CVD TiN coatings for wear-resistant applications: Deposition processes, properties and performance. *Surf. Coat. Technol.* **1994**, *63*, 1–13. [[CrossRef](#)]

2. Zhang, H.; Li, F.; Jia, Q. Preparation of titanium nitride ultrafine powders by sol-gel and microwave carbo-thermal reduction nitridation methods. *Ceram. Int.* **2009**, *35*, 1071–1075. [[CrossRef](#)]
3. Ehiasarian, A.; Vetushka, A.; Gonzalvo, Y.A.; Sáfrán, G.; Székely, L.; Barna, P.B. Influence of high power impulse magnetron sputtering plasma ionization on the microstructure of TiN thin films. *J. Appl. Phys.* **2011**, *109*, 104314. [[CrossRef](#)]
4. Sato, M.; Kitada, H.; Takeyama, M.B. Characterization of TiN films sputter-deposited at low temperatures for Cu-through-silicon via. *Jpn. J. Appl. Phys.* **2019**, *58*, SBBC03. [[CrossRef](#)]
5. Chuang, K.-L.; Tsai, M.-T.; Lu, F.-H. Morphology control of conductive TiN films produced by air-based magnetron sputtering. *Surf. Coat. Technol.* **2018**, *350*, 1091–1097. [[CrossRef](#)]
6. Xu, Z.; Zhang, Z.; Bartosik, M.; Zhang, Y.; Mayrhofer, P.H.; He, Y. Insight into the structural evolution during TiN film growth via atomic resolution TEM. *J. Alloys Compd.* **2018**, *754*, 257–267. [[CrossRef](#)]
7. Shin, H.; Kim, H.-I.; Chung, D.Y.; Yoo, J.M.; Weon, S.; Choi, W.; Sung, Y.-E. Scaffold-Like Titanium Nitride Nanotubes with a Highly Conductive Porous Architecture as a Nanoparticle Catalyst Support for Oxygen Reduction. *ACS Catal.* **2016**, *6*, 3914–3920. [[CrossRef](#)]
8. White, N.; Campbell, A.L.; Grant, J.T.; Pachter, R.; Eyink, K.; Jakubiak, R.; Martinez, G.; Ramana, C.V. Surface/interface analysis and optical properties of RF sputter-deposited nanocrystalline titanium nitride thin films. *Appl. Surf. Sci.* **2014**, *292*, 74–85. [[CrossRef](#)]
9. Krawczyk, M.; Lisowski, W.; Sobczak, J.W.; Kosiński, A.; Jablonski, A. Studies of the hot-pressed TiN material by electron spectroscopies. *J. Alloys Compd.* **2013**, *546*, 280–285. [[CrossRef](#)]
10. Chan, M.-H.; Lu, F.-H. Air-based deposition and processing windows of sputtered TiN, TiN_xO_y, and N-doped TiO_x thin films. *Surf. Coat. Technol.* **2012**, *210*, 135–141. [[CrossRef](#)]
11. Kikicaslan, A.; Zabeida, O.; Bousser, E.; Schmitt, T.; Kemberg-Sapieha, J.E.; Martinu, L. Hard titanium nitride coating deposition inside narrow tubes using pulsed DC PECVD processes. *Surf. Coat. Technol.* **2019**, *377*, 124894. [[CrossRef](#)]
12. Krylov, I.; Xu, X.; Qi, Y.; Weinfeld, K.; Korchnoy, V.; Eizenberg, M.; Ritter, D. Effect of the substrate on structure and properties of titanium nitride films grown by plasma enhanced atomic layer deposition. *J. Vac. Sci. Technol. A* **2019**, *37*, 060905. [[CrossRef](#)]
13. Wang, S.-Q. Reactively sputtered TiN as a diffusion barrier between Cu and Si. *J. Appl. Phys.* **1990**, *68*, 5176–5187. [[CrossRef](#)]
14. Gagnon, G.; Currie, J.F.; Brebner, J.L.; Darwall, T. Efficiency of TiN diffusion barrier between Al and Si prepared by reactive evaporation and rapid thermal annealing. *J. Appl. Phys.* **1996**, *79*, 7612–7620. [[CrossRef](#)]
15. Sato, M.; Takeyama, M.B. Relationship between TiN films with different orientations and their barrier properties. *Jpn. J. Appl. Phys.* **2018**, *57*, 07MB01. [[CrossRef](#)]
16. Cheng, P.; DelaCuruz, S.; Tsai, D.; Wang, Z.; Carraro, C.; Maboudian, R. Enhanced thermal stability by introducing TiN diffusion barrier layer between W and SiC. *J. Am. Ceram. Soc.* **2019**, *102*, 5613–5619. [[CrossRef](#)]
17. Sundgren, J.-E. Structure and properties of TiN coatings. *Thin Solid Film.* **1985**, *128*, 21–44. [[CrossRef](#)]
18. Mezger, P.R.; Creugers, N.H. Titanium nitride coatings in clinical dentistry. *J. Dent.* **1992**, *20*, 342–344. [[CrossRef](#)]
19. Al Jabbari, Y.S.; Fehrman, J.; Barnes, A.C.; Zapf, A.M.; Zinelis, S.; Berzins, D.W. Titanium Nitride and Nitrogen Ion Implanted Coated Dental Materials. *Coatings* **2012**, *2*, 160–178. [[CrossRef](#)]
20. Martinez, G.; Shutthanandan, V.; Thevuthasan, S.; Chessa, J.F.; Ramana, C.V. Effect of thickness on the structure, composition and properties of titanium nitride nano-coatings. *Ceram. Int.* **2014**, *40*, 5757–5764. [[CrossRef](#)]
21. Van Bui, H.; Kovalgyn, A.Y.; Wolters, W.A.M. On the difference between optically and electrically determined resistivity of ultra-thin titanium nitride films. *Appl. Surf. Sci.* **2012**, *269*, 45–49. [[CrossRef](#)]
22. Zhang, Y.; Sahasrabudhe, H.; Bandyopadhyay, A. Additive manufacturing of Ti-Si-N ceramic coatings on titanium. *Appl. Surf. Sci.* **2015**, *346*, 428–437. [[CrossRef](#)]
23. Takizawa, H.; Iwasaki, M.; Kimura, T.; Fujiwara, A.; Haze, N.; Endo, T. Synthesis of Inorganic Materials by 28 GHz Microwave Irradiation. *Trans. Mater. Res. Soc. Jpn.* **2002**, *27*, 51–54.
24. Takizawa, H.; Hayashida, C.; Hayashi, Y. Millimeter-wave processing of metals and intermetallic compounds. *Mater. Jpn.* **2006**, *45*, 577–580. (In Japanese) [[CrossRef](#)]

25. Kashimura, K.; Fukushima, J.; Mitani, T.; Sato, M.; Shinohara, N. Metal Ti-Cr Alloy Powders Nitriding under Atmospheric Pressure by Microwave Heating. *J. Alloy. Compd.* **2013**, *550*, 239–244. [[CrossRef](#)]
26. Roy, R.; Agrawal, D.; Cheng, J.; Gedevarishvili, S. Full sintering of powdered-metal bodies in a microwave field. *Nature* **1999**, *399*, 668–670. [[CrossRef](#)]
27. Takayama, S.; Link, D.; Miksch, S.; Sato, M.; Thumm, M. Millimetre wave effects on sintering behaviour of metal powder compacts. *Powder Metall.* **2006**, *49*, 274–280. [[CrossRef](#)]
28. Suzuki, M.; Ignatenko, M.; Yamashiro, M.; Tanaka, M.; Sato, M. Numerical study of microwave heating of micrometer size metal particles. *ISIJ Int.* **2008**, *48*, 681–684. [[CrossRef](#)]
29. Kashimura, K.; Fukushima, J.; Sato, M. Oxygen Partial Pressure Change with Metal Titanium Powder Nitriding under Microwave Heating. *ISIJ Int.* **2011**, *51*, 181–185. [[CrossRef](#)]
30. Fukushima, J.; Kashimura, K.; Takayama, S.; Sato, M. Microwave-energy Distribution for Reduction and Decrystallization of Titanium Oxides. *Chem. Lett.* **2012**, *41*, 39–41. [[CrossRef](#)]
31. Fukushima, J.; Kashimura, K.; Takayama, S.; Sato, M.; Sano, S.; Hayashi, Y.; Takizawa, H. In-Situ Kinetic Study on Non-Thermal Reduction Reaction of CuO during Microwave Heating. *Mater. Lett.* **2013**, *91*, 252–254. [[CrossRef](#)]
32. Goto, H.; Fukushima, J.; Takizawa, H. Control of Magnetic Properties of NiMn₂O₄ by a Microwave Magnetic Field under Air. *Materials* **2016**, *9*, 169. [[CrossRef](#)] [[PubMed](#)]
33. Fukushima, J.; Takayama, S.; Goto, H.; Sato, M.; Takizawa, H. In situ Analysis of Reaction Kinetics of Reduction Promotion of NiMn₂O₄ under Microwave H-Field Irradiation. *Phys. Chem. Chem. Phys.* **2017**, *19*, 17904–17908. [[CrossRef](#)] [[PubMed](#)]



© 2019 by the authors. Licensee MDPI, Basel, Switzerland. This article is an open access article distributed under the terms and conditions of the Creative Commons Attribution (CC BY) license (<http://creativecommons.org/licenses/by/4.0/>).